Biochimica et Biophysica Acta 1777 (2008) 1355–1363

Contents lists available at ScienceDirect

Biochimica et Biophysica Acta

journal homepage: www.elsevier.com/locate/bbabio

Spectroscopic properties of the peridinins involved in chlorophyll triplet quenching in high-salt peridinin–chlorophyll *a*-protein from *Amphidinium carterae* as revealed by optically detected magnetic resonance, pulse EPR and pulse ENDOR spectroscopies

Marilena Di Valentin [a], Stefano Ceola [a], Enrico Salvadori [a], Giancarlo Agostini [c], Giorgio Mario Giacometti [b], Donatella Carbonera [a,*]

[a] *Dipartimento di Scienze Chimiche, Università di Padova, via Marzolo 1, 35131 Padova, Italy*
[b] *Dipartimento di Biologia, Università di Padova, vi U. Bassi, 35131 Padova, Italy*
[c] *CNR, Istituto di Chimica Biomolecolare, Sezione di Padova, via Marzolo 1, 35131 Padova, Italy*

ARTICLE INFO

Article history:
Received 7 May 2008
Received in revised form 6 June 2008
Accepted 6 June 2008
Available online 18 June 2008

Keywords:
Peridinin
Carotenoid
Triplet
ODMR
EPR
ENDOR
HSPCP
MFPCP

ABSTRACT

The photoexcited triplet state of the carotenoid peridinin in the high-salt peridinin–chlorophyll *a*-protein (HSPCP) of the dinoflagellate *Amphidinium carterae* was investigated by ODMR (optically detected magnetic resonance), pulse EPR and pulse ENDOR spectroscopies. The properties of peridinins associated to the triplet state formation in HSPCP were compared to those of peridinins involved in triplet state population in the main-form peridinin–chlorophyll protein (MFPCP), previously reported. In HSPCP no signals due to the presence of chlorophyll triplet state have been detected, during either steady-state illumination or laser-pulse excitation, meaning that peridinins play the photo-protective role with 100% efficiency as in MFPCP. The general spectroscopic features of the peridinin triplet state are very similar in the two complexes and allow drawing the conclusion that the triplet formation pathway and the triplet localization in one specific peridinin in each subcluster are the same in HSPCP and MFPCP. However some significant differences also emerged from the analysis of the spectra. Zero field splitting parameters of the peridinin triplet states are slightly smaller in HSPCP and small changes are also observed for the hyperfine splittings measured by pulse ENDOR and assigned to the β-protons belonging to one of the two methyl groups present in the conjugated chain, (a_{iso} = 10.3 MHz in HSPCP vs a_{iso} = 10.6 MHz in MFPCP). The differences are explained in terms of local distortion of the tails of the conjugated chains of the peridinin molecules, in agreement with the conformational data resulting from the X-ray structures of the two complexes.

1. Introduction

The water soluble peridinin–chlorophyll *a*-protein (PCP) of the dinoflagellate *Amphidinium carterae*, belongs to the group of marine eukaryotic algae which employ carotenoids, such as peridinin, characterized by the presence of a carbonyl group in their molecular structure, to fulfil the light-harvesting function during photosynthesis.

The main-form PCP, MFPCP, contains peridinin and chlorophyll (Chl) *a* molecules in a stoichiometric ratio of 4:1 [1]. Along with the MFPCP, a minor component has also been isolated from *A. carterae*, which is eluted from an anion exchange column at high-salt concentration [2]. This form is denoted high-salt PCP (HSPCP) and presents 31% identity in amino acid sequence with MFPCP. It contains only six peridinins and two Chl *a* molecules and presents a larger number of positively charged amino acid residues.

The X-ray structure of MFPCP from *A. carterae* has been resolved to 2.0 Å [1]. The basic structure is a trimer. In each subunit of the trimer the pigments are arranged as two pseudo-identical domains of four peridinins and one Chl *a* molecule, as shown in Fig. 1. The pigments are located in the hydrophobic cavity formed by the protein. The peptide primary sequences of the $-NH_2$ and −COOH terminal regions are largely (56%) homologous and form structurally almost identical domains, each consisting of eight alpha-helices. The MFPCP complex has a molecular weight of 32 kDa. Distances between peridinins

Abbreviations: PID, peridinin; Chl, chlorophyll; PCP, peridinin–chlorophyll protein; *A. carterae*, *Amphidinium carterae*; MFPCP, main-form PCP; HSPCP, high-salt PCP; ODMR, optically detected magnetic resonance; FDMR, fluorescence detected magnetic resonance; ADMR, absorption detected magnetic resonance; ZFS, zero field splitting; ISC, intersystem crossing; ESE, electron spin echo; ENDOR, electron nuclear double resonance; TR-EPR, Time-resolved Electron Paramagnetic Resonance; hf: hyperfine; hfcs: hyperfine constants

* Corresponding author. Tel.: +39 049 827 5144; fax: +39 049 827 5161.
E-mail address: donatella.carbonera@unipd.it (D. Carbonera).

0005-2728/$ – see front matter © 2008 Elsevier B.V. All rights reserved.
doi:10.1016/j.bbabio.2008.06.006

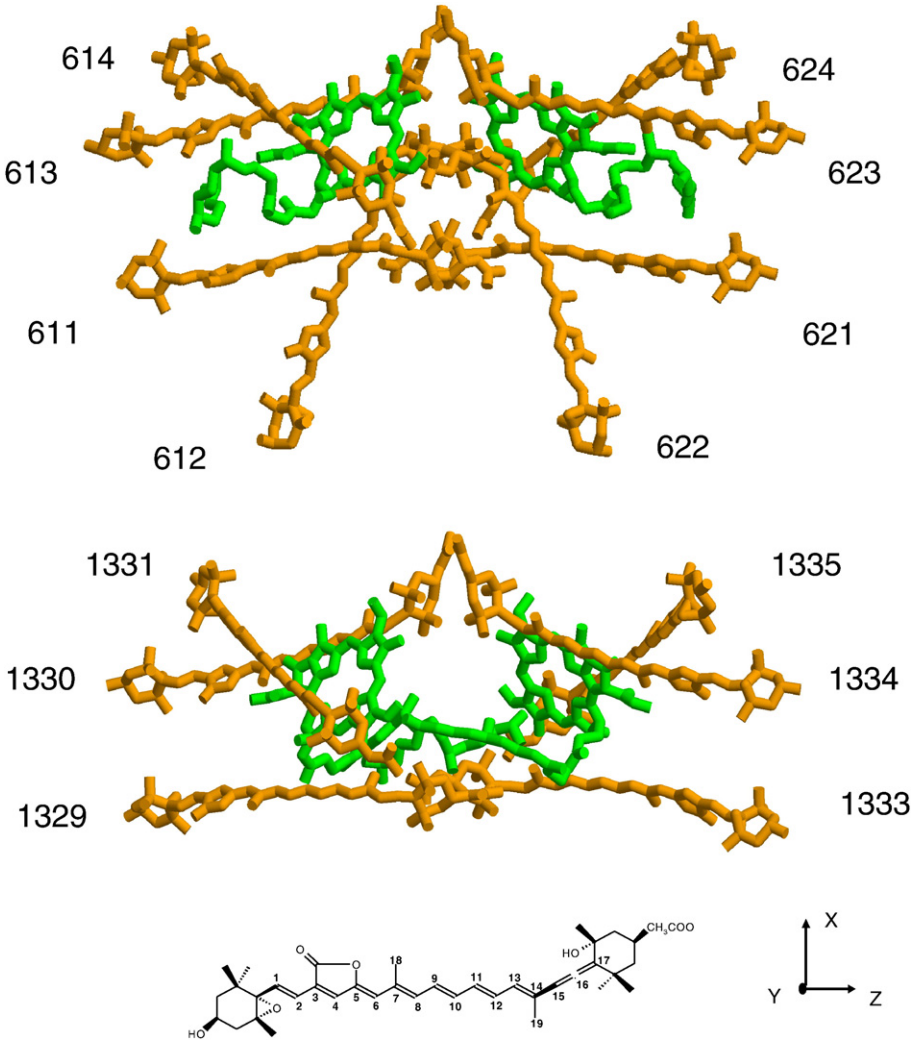

Fig. 1. (Top) Structure of the pigments associated with the monomeric basic unit of the PCP complex from *A. carterae*. Structure taken from coordinates of MFPCP complex 1PPR deposited in the Brookhaven Protein Data Bank. The numbers refer to the peridinins in the PDB files, the numbering is maintained. (Bottom) Structure of the pigments associated with the monomeric basic unit of the HSPCP complex from *A. carterae*. Structure taken from coordinates of PCP complex 2C9E deposited in the Brookhaven Protein Data Bank. The molecular structure of peridinin with the numbering of atoms and the orientation of the ZFS tensor axes is also reported.

within a single domain range from 4 to 11 Å, and the conjugated regions of the peridinins are in van der Waals contact (3.3–3.8 Å) with the tetrapyrrole rings of the Chl *a* molecules. The distance between the Mg atoms of the two Chl *a* molecules in each subunit is 17.4 Å.

Recently, the X-ray structure of HSPCP, which has a molecular weight of 34 kDa, has also been determined (T. Schulte, F.P. Sharples, R.G. Hiller, E. Hofmann, Coordinates have been deposited in the Brookhaven Protein Data Bank under ID 2C9E, unpublished) [3]. It shows a large similarity with the MFPCP structure in terms of pigment arrangement, except for the absence of two symmetry related peridinins, called PID612/PID622, according to the nomenclature of Hofmann et al. [1]. These two peridinins have been proposed to have blue-shifted absorption in the MFPCP complex [4]. An interesting difference between MFPCP and HSPCP complexes is the distance between the Mg atoms of the two Chl *a* molecules in each subunit, which is larger in the HSPCP complex (18.4 Å). Moreover, in HSPCP the phytol tails are located in the space between the two Chls, whereas in MFPCP they point to the external part of the protein. A direct comparison of the pigment arrangement in the structure of MFPCP and HSPCP is shown in Fig. 1. The different local environment of the two Chl molecules in the HSPCP complex leads to a splitting of the Chl *a* Qy absorption band at low temperature which is not observed in MFPCP [4].

After the publication of the X-ray structure of MFPCP, the number of spectroscopic studies and quantum mechanical calculations, aimed to correlate the spectroscopic properties to the arrangement of the pigments in the protein, increased quickly. Recently the study has been extended also to HSPCP which was investigated using absorption, fluorescence, fluorescence excitation, two-photon, and fast-transient optical spectroscopy [3,4]. Absorption spectra of both complexes were recorded at 10 K and analyzed in the 400–600 nm region by summing the individual 10 K spectra of Chl *a* and peridinin recorded in 2-MTHF. Fluorescence excitation spectroscopy revealed a high peridinin-to-Chl *a* energy transfer efficiency (>95%) [4]. Femtosecond time-resolved optical methods have been used to compare the energy transfer dynamics in MFPCP and HSPCP. The Chl-to-Chl energy transfer rate constant for MFPCP was found to be a factor of 4.2 larger [3].

It is well known that carotenoids bound to the light-harvesting complexes of bacteria, plants and algae, and having more than seven double bonds in the conjugated polyene chain, possess low-lying triplet states capable of trapping (B) Chl *a* triplet states, avoiding in this way the formation of potentially harmful singlet oxygen, and are able to quench active oxygen species [5]. Peridinin molecules in the isolated MFPCP complex are able to play this photo-protective role, with a 100% efficiency in terms of triplet–triplet energy transfer. The lifetime of the Chl *a* triplet state is of the order of 20 ns, within this

time a triplet state is formed on the circumferential peridinins and decays through radiationless intersystem crossing channels with a lifetime of 10 μs at room temperature [6].

In the past we used ODMR (optically detected magnetic resonance) to study the formation of triplet state in isolated MFPCP complexes [7–9]. The technique is particularly powerful in the study of photoinduced triplet states because it allows correlating the magnetic properties of the triplet state with the optical properties of the system. More recently, in a time-resolved EPR (TR-EPR) work on the peridinin triplet state generated in PCP proteins from *A. carterae*, we exploited the concept of spin conservation during triplet–triplet energy transfer, to identify the peridinin–chlorophyll pairs directly involved in the triplet energy transfer. By comparing the TR-EPR spectra of MFPCP and HSPCP and their X-ray structures, we suggested that the pathway of triplet quenching and triplet localization was quite similar in the two complexes [10]. We performed also pulse EPR and pulse ENDOR experiments on MFPCP at variable temperatures [11]. The ENDOR investigation, accompanied by DFT calculation of the hyperfine couplings, strongly supported the hypothesis of localization of the triplet state on one peridinin in each subcluster of MFPCP.

The triplet state of peridinins in HSPCP has not been characterized at the same extent. In this paper we complete the investigation on HSPCP and present an extended magnetic resonance study by using several techniques, namely ODMR, electron spin echo (ESE) and pulse ENDOR.

The results are compared to those previously obtained for MFPCP and discussed in terms of energy transfer properties, specific pathway for triplet quenching and protein structure.

2. Materials and methods

2.1. Sample preparation

The MFPCP and HSPCP complexes, extracted and purified according to Sharples et al. [2], were kindly supplied by R.G. Hiller.

2.2. Spectroscopic methods

2.2.1. ODMR and fluorescence experiments

The samples were diluted to a final Chl concentration equivalent to 100 μg/ml and 60% v/v glycerol was added in order to obtain a transparent glass upon cooling of the sample to the cryogenic temperature of the experiments. Fluorescence detected magnetic resonance (FDMR) and absorption detected magnetic resonance (ADMR) experiments were performed in the same laboratory build apparatus, previously described in detail [12,13]. The flexibility of the set up allows performing both kinds of experiments on the same sample by switching the detection mode. Briefly, ODMR is a double resonance technique based on the simple principle that, when upon illumination a triplet steady-state population is generated in a system, the application of a resonant microwave electromagnetic field between a couple of spin sublevels of the triplet state, generally induces a change of the steady-state population of the triplet state itself, due to the anisotropy of the decay and population rates of the three spin sublevels. The induced change of the triplet population may be detected as a corresponding change of the emission and/or absorption of the system [14,15]. Amplitude modulation of the applied microwave field is used to greatly increase the signal to noise ratio by means of a phase sensitive lock-in amplifier (EG&G 5220). In the FDMR experiments the fluorescence, excited by a halogen lamp (250 W) focused into the sample and filtered by a broadband 5 cm solution of $CuSO_4$ 1 M, was collected at 45 degrees through appropriate band-pass filters (10 nm FWHM) by a photodiode before entering the lock-in amplifier. Low temperature emission spectra were detected in the same apparatus used for ODMR experiments, using the same excitation source, but substituting the band-pass filters before the photodiode, coupled to a voltage-amplifier, by a monochromator.

In the absorption detection mode (ADMR) the same excitation lamp was used but without filters before the sample, except for 5 cm water and heat filters. The beam was focused into the monochromator after passing the sample and finally collected by a photodiode. The modulation frequency and the microwave power were chosen depending on the experiment. By fixing the microwave frequency at a resonant value while sweeping the detection wavelength, microwave-induced triplet-minus-singlet (T−S) spectra can be registered.

The temperature was 1.8 K. At such a temperature spin-lattice relaxation is inhibited and the ODMR signal is intense. In the experiments at higher temperatures the helium flow in the cryostat was adjusted to obtain a stable temperature.

2.2.2. Pulse EPR and pulse ENDOR experiments

The concentration of the samples was 1.0 mg protein/ml. Oxygen was removed from the samples by flushing argon in the capillary before freezing. Glycerol, previously degassed by several cycles of freezing and pumping, was added (60%v/v) to obtain a transparent matrix.

Experiments were performed on a Bruker Elexsys E580 pulsed EPR spectrometer equipped with a Bruker ENDOR accessory (E560D-P) and a radio frequency amplifier (AR751 — 150 W). Laser excitation at 532 nm (10 mJ per pulse and repetition rate of 10 Hz) was provided by the second harmonic of a Nd:YAG laser (Quantel Brilliant) in the optically transparent dielectric ring ENDOR resonator (EN4118X-MD4). The temperature was controlled with a Helium cryostat (Oxford CF935) driven by a temperature controller (Oxford ITC503).

Field-swept ESE spectra were recorded using a 2-pulse ESE sequence according to the scheme: flash-DAF-π/2-τ-π-τ-echo (DAF = delay after laser flash). ESE-detected kinetics at the triplet canonical orientations were recorded using a 2-pulse (flash-DAF-π/2-τ-π-τ-echo) ESE sequence after a variable DAF (500 ns step) between the laser flash and the first MW pulse. The π/2-pulse was of 16 ns and the delay τ was set at 200 ns for the field-swept ESE experiment and to 120 ns for the ESE-detected kinetics.

Mims ENDOR experiments were recorded using the MW pulse sequence flash-DAF-π/2-τ-π/2-T-π/2, with 16 ns pulse duration, in conjunction with an RF pulse of 3 μs duration, starting 0.3 μs after the second MW pulse. The DAF was 50 ns, the delay τ was variable, and the time T was 3.8 μs to accommodate the RF pulse. Mims ENDOR spectra were recorded at different τ values (from 160 ns to 240 ns) and added together to eliminate τ dependent blind spots. Pulse ENDOR spectra were accumulated for ≈15 h.

Simulations of the field-swept ESE spectra and DAF kinetics were performed according to the method previously described in Ref. [11].

3. Results

The absorption spectrum of HSPCP, taken at room temperature, was identical to the one reported by Ilagan et al. [4]. At cryogenic temperatures the splitting of the Qy band of the Chl *a* and a red shift of the carotenoid absorption in the region 450–550 nm, when compared to MFPCP, were observed, as previously reported for spectra detected at 10 K [4]. At 1.8 K the fluorescence emission maximum was at 677 nm, 2 nm red-shifted compared to the value reported for the emission at 77 K [4]. In Fig. 2, the emission spectrum at 1.8 K is shown.

3.1. Odmr

Steady-state illumination of the sample at cryogenic temperatures induces the formation of triplet states which can be detected by monitoring the change of the emission of the sample while sweeping the microwave field in the spectral region where chlorophyll and carotenoid triplet states are expected to show resonant transitions

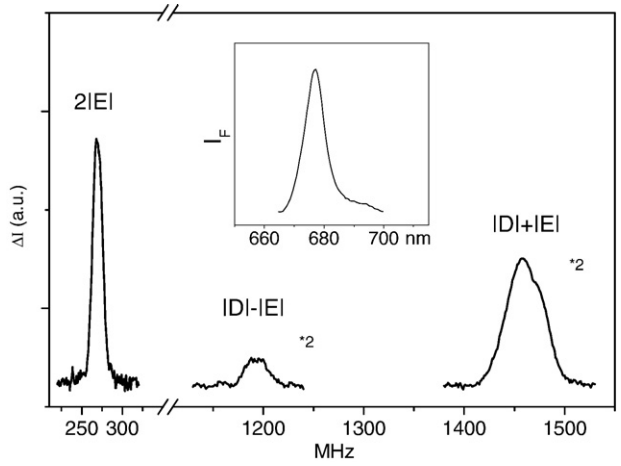

Fig. 2. FDMR spectra of peridinin triplet state in HSPCP at 1.8 K. Detection wavelength: 680 nm; modulation frequency: 323 Hz, microwave power: 1 W, 10 scans. Inset: Fluorescence emission spectra of HSPCP at 1.8 K.

between couples of spin sublevels. In principle, FDMR should not be suitable for detection of carotenoid triplet states, since carotenoids are non-fluorescing molecules. However, it has been previously demonstrated [7,16,17] that, due to the energy transfer processes going on among carotenoids and chlorophylls in the antenna complexes, a change of the steady-state population of the carotenoid triplet state, induced by a resonant microwave field, is reflected by a change of the intensity of the emission of the nearby chlorophyll molecules. In Fig. 2 the FDMR spectra, taken at wavelength corresponding to the maximum of the emission spectrum and in the microwave field region where the 2|*E*|, the |*D*|−|*E*| and the |*D*|+|*E*| transitions of carotenoids are expected, are shown. Three transitions with the polarization pattern usually found for carotenoids (intensity of 2|*E*|>> |*D*|+|*E*|>|*D*|+|*E*|) have been detected at 269, 1190 (sh1212) and 1458 (sh1470) MHz, proving the ability of the peridinins in the HSPCP complex to quench Chl triplet states by populating carotenoid triplets, even at very low temperature. The transition frequencies are slightly shifted with respect to those previously reported for MFPCP (i.e. 267, 1203(sh1229), 1465(sh1499) MHz) [7–9]. As found for most ODMR spectra of carotenoids, the |*D*|+|*E*| and |*D*|−|*E*| transitions are largely inhomogeneous. This leads to a decomposition of each triplet transition in at least two main Gaussian components (not shown) as previously found for MFPCP [8]. The resulting two triplet states are characterized by the following zero field splitting (ZFS) parameters: |*D*|=0.0440 cm^{-1}, |*E*|=0.0044 cm^{-1} and |*D*|= 0.0446 cm^{-1}, |*E*|=0.0045 cm^{-1}. The |*D*| values are both smaller than the corresponding values found for the two triplet states detected in MFPCP (|*D*|=0.0448 cm^{-1} |*E*|=0.0044 cm^{-1} and |*D*|=0.04586 cm^{-1} |*E*|= 0.0045 cm^{-1}). The results are collected in Table 1.

No signals which could be ascribed to the presence of unquenched Chl a triplet states have been detected in the steady-state conditions of the experiments, meaning that the efficiency of triplet quenching is 100%, as already found in MFPCP [7].

The microwave-induced T−S spectra taken at the maximum of the intense 2|*E*| transition (269 MHz) and at two different frequencies, chosen in the broad |*D*|+|*E*| transition, are shown in Fig. 3. The main features of the T−S spectra are very similar to those previously reported for MFPCP (thin line in Fig. 3, from [7]). Broad and complex triplet–triplet absorption bands due to peridinin triplet states are present in the whole spectral range from 450 to 650 nm. A remarkable difference is that in HSPCP the bleaching in the Q_y region of Chl *a* absorption splits clearly in two bands: a sharp feature at 675.8 nm and another broader feature at about 670 nm. A single positive band is observed at 678.7 nm. The sharp bleaching is relatively more pronounced when the spectrum is taken at 1476 MHz, in correspondence to the shoulder of the |D|+|E| transition, compared to the spectrum detected at 1457 MHz.

At 130 K and higher temperatures, the T−S spectrum becomes smoother, the sharp negative/positive features in the Q_y region of Chl absorption disappear and only a broad bleaching centred at about 670 nm remains (data not shown).

3.2. ESE and pulse ENDOR

In our previous work on triplet–triplet energy transfer in PCP from *A. carterae* we reported the TR-EPR spectrum of the HSPCP [10] and found that it was very similar to the spectrum of the MFPCP. Here we extend the characterization of the triplet state in terms of ESE and pulse ENDOR spectroscopy and compare the results to those obtained for MFPCP [11].

While kinetic measurements in time-resolved EPR are hampered by the presence of microwave-induced transition probabilities, ESE spectroscopy does not suffer of this complication since in this technique there is no microwave field present in the period between the photogeneration of the triplet state and its detection [18]. The kinetics of population and decay of the triplet spin sublevels, obtained by monitoring the echo intensity as a function of DAF at the low-field canonical orientations of the ZFS tensor (Z^-, Y^+, X^+), are shown in Fig. 4 together with the ESE-detected spectrum at a DAF of 50 ns, at 20 K. Direct comparison with the data on MFPCP taken from Ref. [11] is reported in Fig. 4. Due to the absence of fast and anisotropic relaxation processes depending on the orientation of the triplet state with respect to the magnetic field, the ESE-detected spectra taken at early times after the laser flash are substantially the same, in terms of shape, as the initial TR-EPR spectra previously reported [10].

As observed for MFPCP, the spin polarization varies in time, showing an intensity increase at the *Y* canonical resonance in the first 20 ms. Simulations of the ESE-detected spectra and ESE kinetics, according to the method described in [11], give the ZFS parameters, the relative populating rates and decay rates for the peridinin triplet sublevels in HSPCP reported in Table 1. Simulations of the ESE-detected spectra and ESE kinetics are not shown. The order of the ZFS energy levels is: $Z^2>Y^2>X^2$. As discussed before [10], the corresponding ZFS axes of the peridinin triplet state in the molecular frame are the following: the long axis is the *Z* axis, the *X* axis is along the C–H bonds in the conjugated chain and the *Y* direction is perpendicular to the conjugated *XZ* molecular plane. These axes are shown in the molecular scheme of peridinin reported in Fig. 1.

To search for possible local differences in the triplet electronic distribution of the peridinin(s) where the triplet becomes localized after triplet–triplet transfer from the Chl(s) molecule(s) we performed

Table 1
Parameters of the peridinin triplet state

	|*D*| (10^{-4} cm^{-1})	|*E*| (10^{-4} cm^{-1})	P_X: P_Y: P_Z	k_X: k_Y: k_Z (μs^{-1})	Ref.
MFPCP	449.7±0.1 (ESE)	43.9±0.1 (ESE)	0.18: 0.37: 0.45	0.15: 0.03: 0.09	[11]
	448.0±0.1 (ODMR)	44.0±0.1 (ODMR)			[8]
	458.6±0.1 (ODMR)	45.0±0.1 (ODMR)			[8]
HSPCP	443.6±0.1 (ESE)	45.1±0.1 (ESE)	0.18: 0.39: 0.43	0.135: 0.028: 0.08	
	440.0±0.1 (ODMR)	44.6±0.1 (ODMR)			
	446.0±0.1 (ODMR)	45.0±0.1 (ODMR)			

Values of the relative population rates, P_X, P_Y and P_Z, and decay constants, k_X, k_Y and k_Z, of the triplet sublevels together with the ZFS parameters |*D*| and |*E*|, derived from simulation of the time evolution of the field-swept ESE spectrum of HSPCP, according to the method described in Ref. [11]. For comparison the data relative to MFPCP from Ref. [11] are also reported. ZFS parameters resulting from the decomposition of the ODMR spectra of HSPCP with Gaussian components are also reported and compared to the equivalent data for MFPCP from Ref. [8]; line widths used in the decomposition were 8, 13, 25 MHz for both the Gaussian components contributing to each of the 2|*E*|, |*D*|−|*E*| and |*D*|+|*E*| transitions respectively.

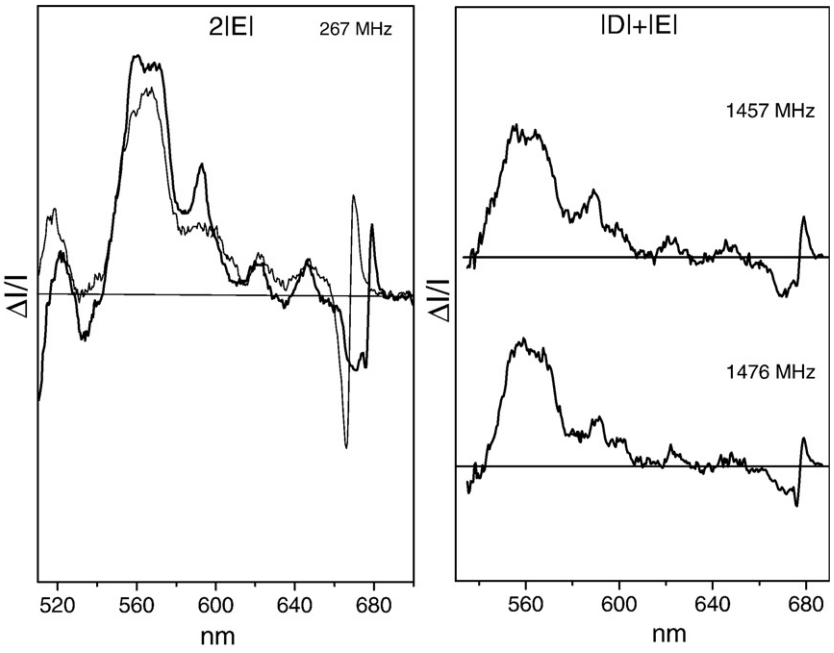

Fig. 3. T−S spectra of HSPCP detected at different resonant microwave frequencies. (Left) Comparison of the T−S spectra of HSPCP (thick line) and MFPCP (thin line) detected at the 2|*E*| transition frequency. Spectra have been rescaled to better comparison. Line corresponding to $\Delta I/I=0$ is shown. (Right) T−S spectra of HSPCP at two frequencies of the broad |*D*+|*E*| transition, as indicated. Lines corresponding to $\Delta I/I=0$ are shown. Modulation frequency: 323 Hz, microwave power: 1 W, $T=1.8$ K. Data relative to MFPCP are identical to those reported in [7]. $\Delta I/I \cong \Delta A$.

time-resolved ENDOR experiments on the triplet state and compared the results to those relative to MFPCP reported in [11]. The measurements of the ENDOR effect at the canonical magnetic field positions shown in the spectrum reported in Fig. 4, give the *Aii* hyperfine tensor components of protons in the reference frame of the ZFS tensor. These hyperfine couplings (hfc) are sensitive probe of the electronic distribution in the conjugated chain. In Fig. 5 the experimental Mims ENDOR spectra of the photoexcited triplet state of peridinin in HSPCP from *A. carterae*, at the X^+/X^- and Z^+/Z^- EPR field positions, obtained at 20 K at early times after the laser flash, are reported and compared to the corresponding spectra for MFPCP [11]. The ENDOR spectra of the Y^+/Y^- EPR field positions show an unstructured line at ν_H (the proton Larmor frequency) at short time and only spectra taken after 18 μs after the laser flash show some significant transitions. The spectrum at the Y^- field position is shown in Fig. 5 while the spectrum at the Y^+ position is omitted because it does not give any additional information showing only weak transitions due to the methyl couplings.

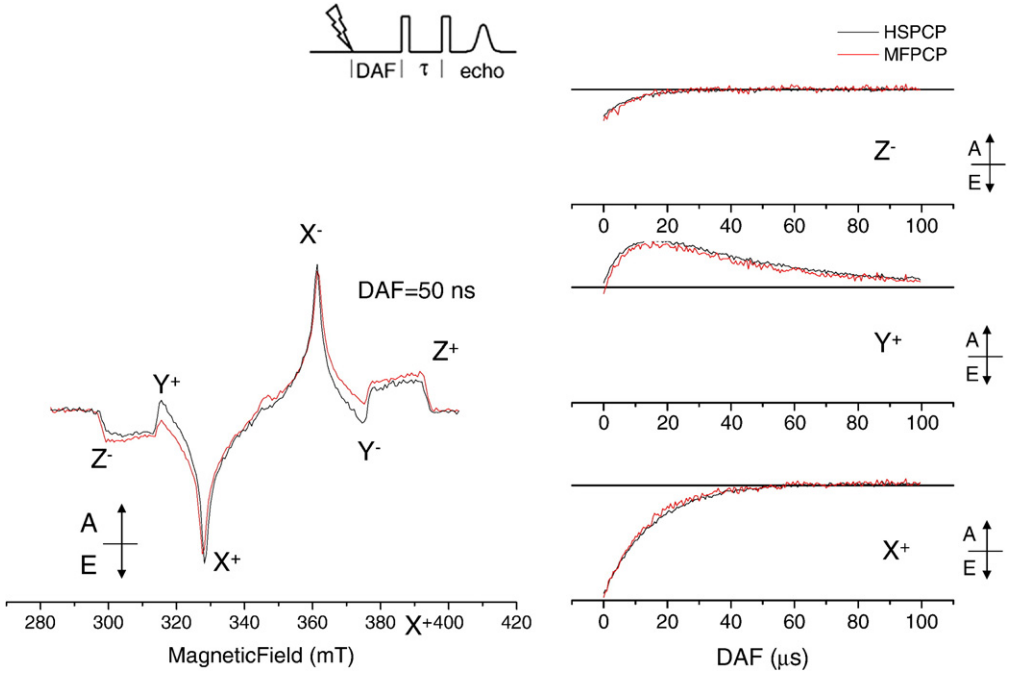

Fig. 4. (Left) Field-swept ESE spectrum of HSPCP (black) and MFPCP (red) from *A. carterae*, at $T=20$ K, at DAF=50 ns. (Right) ESE-detected kinetics, at $T=20$ K, at the low-field canonical fields Z^-, Y^+, X^+ (HSPCP: black lines; MFPCP: red lines). A = absorption, E = emission. For experimental conditions see Materials and methods. Inset: Pulse scheme of the ESE experiment for photoexcited triplet states. Order of energy for zero field triplet sublevels: $|Z|>|X|>|Y|$. Data relative to MFPCP are the same as in Ref. [11].

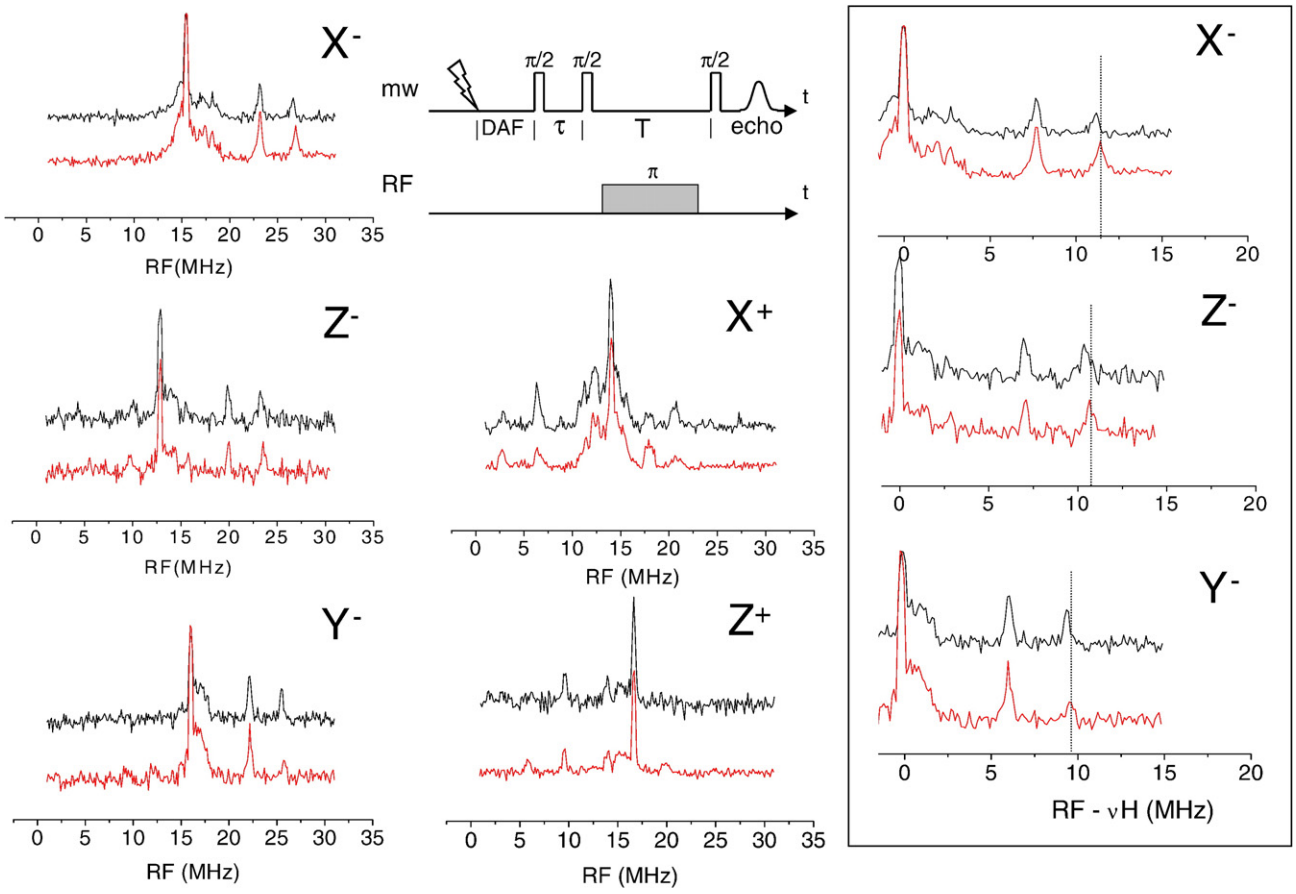

Fig. 5. Pulse Mims ENDOR spectra of HSPCP (black) and MFPCP (red) from *A. carterae* for the *X*, *Y* and *Z* EPR field positions (indicated in Fig. 4) at $T = 20$ K. The ENDOR spectra for the X^+, Y^- and Z^- EPR transitions are in emission but have been inverted for better comparison. The pulse sequence used is indicated. Right panel: region of hfcs relative to the methyl groups enlarged and with a frequency scale which gives the deviation from the ν_H. The hfcs correspond to the frequency shift between the corresponding ENDOR line and the ν_H. For experimental conditions see Materials and methods. Data relative to MFPCP are the same as in Ref. [11].

The two narrow ENDOR transitions, appearing on the low RF (radio frequency) side from ν_H in the X^+ and Z^+ spectra and on the high RF side from ν_H in the X^- and Z^- spectra, correspond to positive hfcs which have been assigned to rotating methyl group at positions 18 and 19 in the molecular structure shown in Fig. 1 [11]. In HSPCP one of the two methyl groups shows hyperfine couplings which are smaller compared to the values found in MFPCP ($A_{XX} = 11.1$ MHz/$A_{YY} = 9.5$ MHz/$A_{ZZ} = 10.3$ MHz versus $A_{XX} = 11.4$ MHz/$A_{YY} = 9.8$ MHz/$A_{ZZ} = 10.7$ MHz), while the other methyl shows the same hfc values: $A_{XX} = 7.6$ MHz, $A_{YY} = 6.2$ MHz $A_{ZZ} = 7.1$ MHz. The values of the hfcs along the three ZFS directions lead to estimate an $a_{iso} = 10.3$ MHz for HSPCP, to be compared to the value 10.6 MHz previously found for MFPCP. In Fig. 5 the ENDOR transitions assigned to the methyl protons, for the three canonical orientations, are shown in a scale (RF-ν_H) which allows the direct estimation of the couplings.

The use of Mims ENDOR was aimed to detect the small hyperfine couplings with more sensitivity to search for possible differences between the two complexes also in the region close to ν_H. However no significant differences were observed in this region. The Davies ENDOR spectra performed on the samples did not give additional information (not shown).

4. Discussion

In HSPCP, peridinins play the photo-protective role with 100% efficiency as in MFPCP. In both complexes no signals due to the presence of chlorophyll triplet state have been detected, during either steady-state illumination or laser-pulse excitation.

Triplet–triplet energy transfer has a very stringent distance requirement and is very sensitive to the mutual orientation of the molecular π orbitals of the molecules involved. In our previous work on MFPCP we have shown that localization of the triplet state mainly in one peridinin in each subcluster is likely to occur [10]. The peridinin–chlorophyll pair, directly involved in the triplet–triplet energy transfer, coincides with the one having the shortest centre to centre distance and the water molecule, which is coordinated to the central Mg atom of the Chl *a* molecule, placed at the interface between the two pigments (PID614/624 in Fig. 1). In our analysis of the TR-EPR data, in terms of triplet–triplet transfer, also PID612 and PID622 resulted to be possible sites of Chl triplet quenching in MFPCP. However, their involvement was supposed to be inessential on the basis of the comparison of the TR-EPR spectra of MFPCP with those obtained for HSPCP because in the latter the analogous of the PID612/622 couple is missing but the TR-EPR spectrum is very similar to that of MFPCP [10]. While the polarization pattern of TR-EPR spectrum of peridinin triplet state is strongly dependent on the relative geometry of the donor-acceptor couple, ODMR and ENDOR spectroscopies are more sensitive to the local environment of the triplet state itself. For this reason we have performed a complete study searching for possible significant differences in triplet localization and molecular environment in HSPCP compared to MFPCP.

4.1. Odmr

The three FDMR transitions are inhomogenously broadened and show two distinct components as previously observed for MFPCP (see

Table 1). The ZFS parameters |*D*| and |*E*| are slightly different in the two complexes; this can be due to the local environment and/or to a distortion of the peridinin molecular skeleton. The two components give a slightly different contribution to the T−S spectrum but overlap at each wavelength. In the TR-EPR and ESE spectra these two components are not distinguishable due to the powder distribution of the anisotropic ZFS tensor and to the hyperfine broadening. The presence of more components with very similar ZFS parameters is a common feature of the ODMR spectra of carotenoid triplet states, in natural systems, taken at very low temperature. We have recently assigned the components to slightly different conformations of the same pigment rather than to different pigments [19,10].

The comparison of the T−S spectra of HSPCP and MFPCP reported in Fig. 3 shows that the general features due to the peridinin triplet states are the same in the two complexes. The main T–T absorption band is centred at about the same wavelength (565 nm) and the red-most bleaching in the peridinin absorption region is observed at about 535 nm in both complexes. In this respect the characteristics of the absorption of the peridinin(s) where the triplet state is localized and the possible interactions with the nearby peridinins, which would be reflected in the T−S spectrum, seem to be similar. Moreover the possibility of a direct involvement of the red-most peridinin of MFPCP, which has been proposed to absorb at 544 nm by Ilagan et al. [3], in the localization of the triplet state may be ruled out because a large difference in the T−S spectra should be expected, being this red absorption absent in HSPCP [3]. On the contrary they are very similar.

Some significant differences are present in the T−S spectrum of the two complexes in the region of the Qy absorption bands of the Chls. The bleaching observed in this region has been assigned to a change in the interaction between peridinin and Chl which takes place when the carotenoid changes the electronic state (from singlet to triplet). This is a common feature observed in all the T−S spectra of carotenoids in natural photosystems reported up to date [19–22]. It is interesting to note that, at least at 1.8 K, both the Chls of the HSPCP complex contribute to the bleaching in the Qy absorption region. The bleaching of the red-shifted Chl, centred at 676 nm, is very sharp, while the second component is broader and centred at about 670 nm. The observation of the bleaching of both the Chls of the complex seems to indicate that, in the experimental conditions of the ODMR experiments (continuous illumination in the range 400–700 nm), carotenoid triplet states are populated in both the subclusters and are localized in close proximity to the two Chl molecules. A possible different explanation of the observed feature in the T−S spectrum could be the presence of a strongly coupled Chl dimer interacting with the peridinin carrying the triplet state. However, this last possibility must be excluded on the basis of the results reported by Ilagan et al. [3], who showed the presence of distinct spectral forms of Chl in HSPCP, and on the basis of the large distance between the Chls planes resulting from the X-ray structure (18.4 Å centre to centre).

4.2. ESE and pulse ENDOR

The absence of significant differences in the ESE (or in the TR-EPR) spectra taken at initial times after the laser flash and in the kinetics of HSPCP with respect to those of MFPCP, indicates that the peridinins responsible for the Chl quenching in the two clusters of HSPCP are substantially similar to those of MFPCP in terms of relative orientation with the triplet donor, the ^{T}Chl, and in terms of ZFS axes directions in the peridinin molecular structure. As already proposed [10,11], the similarity in the polarization pattern of the spectra and in the pigment arrangement of the two protein complexes, strongly suggests a localization of the triplet state on PID1331/1335, the analogous of PID614/624 in MFPCP (see Fig. 1). For sake of precision and completeness, we performed the calculations of the initial ESE triplet spectra for the triplet–triplet energy transfer from each of the two Chls to the three surrounding peridinins in the symmetry related subclusters of the HSPCP complex. The method, described in detail for MFPCP [10], exploits the concept of spin conservation during the triplet–triplet energy transfer. The acceptor (peridinin) inherits the polarization of the donor in a way which depends on the relative geometrical arrangement of the donor-acceptor couple. Although homologous Chl-peridinin couples in the MFPCP and HSPCP structures are slightly different in terms of relative orientation and carotenoid backbone distortions (see Fig. 6), the calculations show that these differences do not produce any significant effect on the calculated spectra and therefore in the assignment of triplet localization. In fact, the best agreement with the experimental spectrum is obtained for triplet transfer to PID1331 and/or 1335. Details of the calculations are reported in the Supplementary material.

At the temperature of the experiments, 20 K, the Chl–Chl transfer rate of the excitation is fast 20 ps [3] and the probability to form the triplet state is likely higher for the Chl absorbing at about 677 nm (Chl 1327 in the X-ray structure of HSPCP). The prevailing triplet is therefore localized mainly on the PID1331 which is close to Chl1327. However the ODMR results indicate that the possibility to form triplet states in both subclusters is not negligible, at least under continuous illumination. With a pulse duration of laser flash of 9 ns, as that used in the time-resolved and ESE experiments, a contribution to the triplet population coming from Chl 1328 is still plausible. The calculation ESE spectra of PID1335 and PID1331, at short DAF, show that they are almost identical (see the Supplementary material). This means that we are not able to evaluate the relative contribution of these peridinins to the triplet quenching. To similar conclusions lead the analysis of the TR-EPR spectra of MFPCP [10].

Interestingly, the water molecule coordinated to the central Mg of the Chl molecules, which has been suggested to play a key role in the triplet–triplet transfer in MFPCP, is present also in HSPCP, forming a bridge between Chl1327(1328) and PID-1331(1335).

Although similarities between HSPCP and MFPCP in terms of pigment arrangement are clearly found, however, looking carefully to the homologous carotenoids in the respective X-ray structures, it is possible to point out some local different conformations of the peridinins. In particular the differences between the homologous PID614/PID1131 are shown in Fig. 6, where the comparison has been made superimposing the planes of the Chls which are close to these peridinins in the two proteins. In principle, these differences should produce a variation of the ZFS parameters and of the spin density distribution of the associated triplet states. Indeed a decrease of the |D| parameter is observed in the ODMR spectra of HSPCP, showing a possible larger delocalization of the electron density in the molecular skeleton. A measurable decrease of the hyperfine couplings, previously assigned to the protons of the methyl group located in position 19 in the molecular structure (see Fig. 1), has also been detected in the time- resolved ENDOR spectra of the triplet state of HSPCP. The methyl groups have been used in our previous work [11] as markers of the electronic structure of the triplet state and the satisfactory agreement between the experimental and computed hyperfine couplings, assigned to the rotating methyl groups on the conjugated chain, provided a critical test of the triplet state wavefunction. DFT calculations showed that the unpaired spins are quite delocalized over the whole conjugated system, with an alternate spin pattern with positive spin densities alternating with gradually smaller negative spin densities. This alternate pattern is lost in the central region of the conjugated chain where all positive densities are found. Similar description of the spin density distribution in the peridinin triplet state was given by Niklas et al. [23] on the basis of the ENDOR data relative to the reconstituted N-domain of PCP. The decrease of the hfcs observed for methyl 19 in HSPCP compared to the values reported for MFPCP indicates that the tail of the conjugated chain where the allenic group is present is a site of molecular distortion. The calculations have shown that this region of the molecular structure is indeed the more

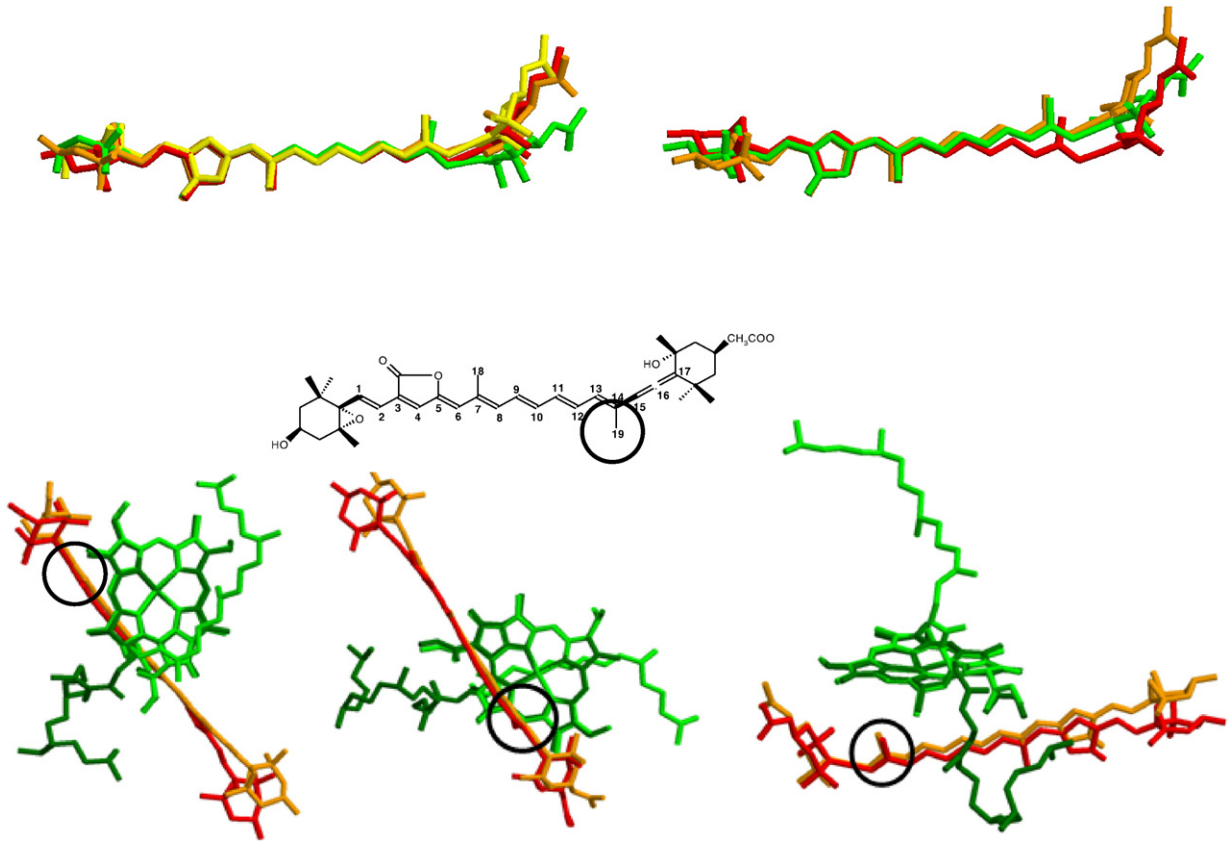

Fig. 6. (Top) Superimposition of the structure of the peridinins associated with one subcluster of MFPCP (left) and HSPCP (right). Green: PID611/1329; yellow: PID612; orange: PID613/1330; red: PID614/1331. (Bottom) Superimposition of the structures of the Chl-PID614 and Chl-PID1331 couples associated with MFPCP and HSPCP respectively. Three different views are shown. Structure taken from coordinates of 1PPR and 2C9E PDB files deposited in the Brookhaven Protein Data Bank. The methyl in position 19 is highlighted both in the molecular structure of peridinin and in the X-ray structures.

affected by conformational disorder [11] as evident also by inspection of Fig. 6 where the superimposition of the peridinins belonging to the same subcluster, of both MFPCP and HSPCP, is shown. The different degrees of bending of the peridinin tails in the conformations assumed by the pigments in the complexes are shown in Fig. 6. The direct comparison between PID614 in MFPCP and PID1331 in HSPCP, which are assumed to be the site of triplet quenching together with PID614 and PID1335, is also shown in Fig. 6. In this figure the methyl group 19 is highlighted by a circle. When the Chl planes relative to the homologous subclusters are superimposed in the two complexes the differences between the peridinins are clearly seen. The methyl in position 18 is located in the central part of the molecules which is more conserved, while methyl 19 is in the region where the two molecules differ the most. On the opposite tail of the molecule there is also a local distortion which should produce a change of the spin density especially at the proton in position 1, where the spin density has been shown to be large from the DFT calculations [11]. Unfortunately the hfcs relative to this proton have not been assigned in our spectra because they have broad transitions which do not easily emerge from the noise. Actually, in the Mims time-resolved ENDOR spectra on the triplet states of the two proteins many expected hfcs are missing, because of the large anisotropy, thus the whole redistribution of the spin density in the skeleton due to the different conformations of the tails cannot be fully described. Nevertheless the methyl marker can be used as evidence of the local distortion of the molecule.

In conclusion, HSPCP and MFPCP share most of the properties relatively to the triplet formation pathway and to the triplet localization in specific peridinins. However some significant differences also emerged from the analysis of the spectra which can be explained in terms of local distortion of the conjugated chains of the peridinins molecules, in agreement with the conformational data resulting from the X-ray structures of the two complexes.

Acknowledgements

This work was supported by the Italian Ministry for University and Research (MURST) under the project PRIN2005. We are grateful to Prof. Giovanni Giacometti for his continuous interest in this work and to Roger Hiller for his interest in the work and for kindly supplying the samples.

Appendix A. Supplementary data

Supplementary data associated with this article can be found, in the online version, at doi:10.1016/j.bbabio.2008.06.006.

References

[1] E. Hofmann, P.M. Wrench, F.P. Sharples, R.G. Hiller, W. Welte, K. Diederichs, Structural basis of light harvesting by carotenoids: peridinin–chlorophyll–protein from *Amphidinium carterae*, Science 272 (1996) 1788–1791.
[2] F.P. Sharples, P.M. Wrench, K.L. Ou, R.G. Hiller, Two distinct forms of the peridinin–chlorophyll alpha-protein from *Amphidinium carterae*, Biochim. Biophys. Acta 1276 (1996) 117–123.
[3] R.P. Ilagan, J.F. Koscielecki, R.G. Hiller, F.P. Sharples, G.N. Gibson, R.R. Birge, H.A. Frank, Femtosecond time-resolved absorption spectroscopy of main-form and high-salt peridinin–chlorophyll proteins at low temperatures, Biochemistry 45 (2006) 14052–14063.
[4] R.P. Ilagan, S. Shima, A. Melkozernov, S. Lin, R.E. Blankenship, F.P. Sharples, R.G. Hiller, R.R. Birge, H.A. Frank, Spectroscopic properties of the main-form and high-

salt peridinin–chlorophyll a proteins from *Amphidinium carterae*, Biochemistry 43 (2004) 1478–1487.
[5] H.A. Frank, R.J. Cogdell, Carotenoids in photosynthesis, Photochem. Photobiol. 63 (1996) 257–264.
[6] J.A. Bautista, R.G. Hiller, F.P. Sharples, D. Gosztola, M. Wasielewski, H.A. Frank, Singlet and triplet energy transfer in the peridinin–chlorophyll a-protein from *Amphidinium carterae*, J. Phys. Chem. A 103 (1999) 2267–2273.
[7] D. Carbonera, G. Giacometti, U. Segre, Carotenoid interactions in peridinin chlorophyll a proteins from dinoflagellates — evidence for optical excitons and triplet migration, J. Chem. Soc. Faraday Trans. 92 (1996) 989–993.
[8] D. Carbonera, G. Giacometti, G. Agostini, FDMR spectroscopy of peridinin chlorophyll-a protein from *Amphidinium-carterae*, Spectrochimica 51A (1995) 115–123.
[9] D. Carbonera, G. Giacometti, U. Segre, A. Angerhofer, U. Gross, Model for triplet–triplet energy transfer in natural clusters of peridinin molecules contained in dinoflagellate's outer antenna proteins, J. Phys. Chem. B 103 (1999) 6357–6362.
[10] M. Di Valentin, S. Ceola, E. Salvadori, G. Agostini, D. Carbonera, Identification by time-resolved EPR of the peridinins directly involved in chlorophyll triplet quenching in the peridinin–chlorophyll a-protein from *Amphidinium carterae*, Biochim. Biophys. Acta 1777 (2008) 186–195.
[11] M. Di Valentin, S. Ceola, G. Agostini, G.M. Giacometti, A. Angerhofer, O. Crescenzi, V. Barone, D. Carbonera, Pulse ENDOR and density functional theory on the peridinin triplet state involved in the photo-protective mechanism in the peridinin–chlorophyll a-protein from *Amphidinium carterae*, Biochim. et Biophys. Acta 1777 (2008) 295–307.
[12] D. Carbonera, G. Giacometti, G. Agostini, FDMR of carotenoid and chlorophyll triplets in light-harvesting complex LHCII of spinach, Appl. Magn. Reson. 3 (1992) 361.
[13] S. Santabarbara, E. Bordignon, R.C. Jennings, D. Carbonera, Chlorophyll triplet states associated with photosystem II of thylakoids, Biochemistry 41 (2002) 8184.
[14] R.H. Clarke, Triplet State ODMR Spectroscopy. Techniques and Applications to Biophysical Systems, in: R.H. Clarke (Ed.), Wiley-Interscience, New York, 1982.
[15] A.J. Hoff, Optically Detected Magnetic Resonance of Triplet States. Advanced EPR, in: A.J. Hoff (Ed.), ELSEVIER, Amsterdam, 1989.
[16] D. Carbonera, G. Giacometti, G. Agostini, A. Angerhofer, V. Aust, ODMR of carotenoid and chlorophyll triplets in CP43 and CP47 complexes of spinach, Chem. Phys. Lett. 194 (1992) 275–281.
[17] D. Carbonera, E. Bordignon, G. Giacometti, G. Agostini, A. Vianelli, Fluorescence and absorption detected magnetic resonance of chlorosomes from green bacteria *Chlorobium tepidum* and *Chloroflexus aurantiacus*. A comparative study, J. Phys. Chem B 105 (2001) 246–255.
[18] T.S. Lin, Electron spin echo spectroscopy of organic triplets, Chem. Rev. 84 (1984) 1–15.
[19] D. Carbonera, G. Agostini, T. Morosinotto, R. Bassi, Quenching of chlorophyll triplet states by carotenoids in reconstituted Lhca4 subunit of peripheral light-harvesting complex of photosystem I, Biochemistry 44 (2005) 8337–8346.
[20] R. Van der Vos, D. Carbonera, A.J. Hoff, Microwave and optical spectroscopy of carotenoid triplets in light-harvesting complex LHCII of spinach by absorbance-detected magnetic resonance, Appl. Magn. Res. 2 (1991) 179–202.
[21] T. Javorfi, G. Garab, K. Razi Naqvi, Reinvestigation of the triplet-minus-singlet spectrum of chloroplasts, Spectrochim. Acta Part A 56 (2000) 211–214.
[22] A. Angerhofer, F. Bornhauser, A. Gall, R.J. Cogdell, Optical and optically detected magnetic resonance investigation on purple photosynthetic bacterial antenna complexes, Chem. Phys. 194 (1995) 259–274.
[23] J. Niklas, T. Schulte, S. Prakash, M. van Gastel, E. Hofmann, W. Lubitz, Spin-density distribution of the carotenoid triplet state in the peridinin–chlorophyll–protein antenna. A Q-band pulse electron-nuclear double resonance and density functional theory study, J. Am. Chem. Soc. 129 (2007) 15442–15443.